Cyclic freeze–thaw behavior of coal gangue based geopolymer

Xiaoyun Yang, Cheng Lin
Department of Civil Engineering – University of Victoria, Victoria, British Columbia, Canada
Xiaoyun Yang
College of Energy and Transportation Engineering – Inner Mongolia Agricultural University, Hohhot, China

GeoCalgary 2022 October 2-5
Reflection on Resources

ABSTRACT
Coal gangue, a solid waste by-product of coal, is a desirable material for making a geopolymer. To promote the application of coal gangue based geopolymer in cold regions, this study investigates the cyclic freeze-thaw responses of the coal gangue based geopolymer, which was activated by NaOH activator, Na_2SiO_3 + NaOH activator and NaOH+Na_2SiO_3+ desulfurized gypsum activator. The appearance, cross-section, mass loss and strengths were measured, and the microscopic mechanism was analyzed by X-Ray diffraction (XRD), Fourier transform infrared spectroscopy (FTIR) and scanning electron microscopy (SEM). Results show that: (1) the surface peeling and the internal crisping of the geopolymers were observed after the freeze-thaw cycles; (2) the SS and SSG geopolymer(activated by NaOH+ Na_2SiO_3 and NaOH+Na_2SiO_3+ desulfurized gypsum, respectively) developed higher freeze-thaw resistance than the SH geopolymer(activated by NaOH); (3) the freeze-thaw resulted in reduced geopolymer gels, increased voids and loosening, but formed no new gels; and (4) SS and SSG geopolymers had high hydration degree and dense than SH geopolymers.

RÉSUMÉ
Le schiste de charbon est un sous-produit des résidus de charbon, idéal pour la fabrication de géopolymères. Afin de faciliter l'utilisation des polymères à base de résidus de charbon dans les régions froides, on a étudié la réponse cyclique des activateurs NaOH, Na_2SiO_3+ NaOH et NaOH+Na_2SiO_3+ désulfuration des gypses aux polymères à base de résidus de charbon. La morphologie, la section transversale, la perte de masse et la résistance ont été déterminées par la diffraction des rayons x (DRX), la spectroscopie infrarouge à transformation de fourier (FTIR) et la microscopie électronique à balayage (mev). 1) l'écaillage et le froissage interne de la surface du géopolymère se produisent après le cycle de gel/dégel; (2) les géopolymères SS et SSG (activés respectivement par NaOH+Na_2SiO_3 et NaOH+Na_2SiO_3+ gypse désulfuré) ont une résistance au gel et au dégel plus élevée que les géopolymères SH (activés par NaOH); (3) le gel et le dégel entraînent une diminution du gel géopolymère, une augmentation de la porosité et un relâchement, mais aucun nouveau gel n'est formé; (4) les géopolymères SS et SSG ont un degré élevé d'hydratation et une plus grande densité que les géopolymères SH.

1 INTRODUCTION

Geopolymer is a kind of environment-friendly environmental material, which is formed from solid waste with high content of silicon and aluminum after alkali solution activation. Geopolymer has been successfully used as construction materials for building floor slabs, airport runways, bridges, 3D printing, quick repair and other engineering applications. For example, the floors of the University of Queensland GCI building were fly ash-based geopolymers (Rligh and Glasby 2013). Slag and fly ash geopolymers with high bending resistance and low cracks were used in the turning nodes, apron and taxiway pavements of Brisbane West Wellcamp Airport (Glasby et al. 2015). Construction and demolition waste-based geopolymer mortars could be used for 3D printing (Ilcan et al. 2022). According to Kantarci and Maraş (2022), mineral powder geopolymer slurries can be used to repair reinforced concrete beams. Although geopolymers have been successfully used in various fields, their long-term behavior such as the freeze-thaw performance, acid and alkali corrosion resistance, dry and wet cycle resistance, is still an ongoing research subject. Sun et al. (2022) studied the life prediction of tailings and waste rock aggregate geopolymer concrete under freeze-thaw cycles and found that geopolymers have excellent freeze-thaw cycle resistance. Bakharev (2005) soaked geopolymer concrete in the sulfuric acid solution for 5 months and concluded that the compressive strength of geopolymer with better performance could still reach more than 30MPa. Dos Santos et al. (2021) studied the dry-wet cycle performance of sisal fiber-reinforced sustainable geopolymer composites and concluded that the flexural strength could still reach 11 MPa after the dry-wet cycle. To promote the use of gangue base polymer in cold areas, this paper measured the appearance of gangue base polymer, changes in cross-section, mass loss, compressive and flexural strength under the influence of the freezing-thawing cycle, and used X-Ray diffraction (XRD), Fourier transform infrared spectroscopy (FTIR), scanning electron microscopy (SEM) to analyze the microscopic mechanism of its freezing-thawing cycle performance.

2 MATERIALS AND METHODS

2.1 Materials

Coal gangue powder and ground granulated blast-furnace slag powder (GGBFS) were obtained from Hejin City, Shanxi Province, China. The raw coal gangue powder is not reactive, so it needs to be crushed, calcined in a muffle furnace at 700°C for 2hrs (Zhu et al. 2020), and ground in a high-speed pulverizer to prepare a highly reactive calcined ultra-fine coal gangue powder (CUCG). The GGBFS grade was Grade 100. the composition of CUCG and GGBFS powder is shown in Table 1. Three activators were selected, namely NaOH activator (SS activator), Na_2SiO_3+NaOH activator (SS activator) and Na_2SiO_3+NaOH+desulfurized gypsum activator (SSG activator).

Table 1. Chemical composition of CUCG and GGBFS powder /%.

Materials	SiO_2	Al_2O_3	Fe_2O_3	CaO	K_2O	TiO_2	MgO	SO_3	Na_2O	Others
CUCG	54.2	41.6	0.98	0.55	0.91	0.96	0.10	0.02	0.46	0.22
GGBFS	34.9	16.7	1.05	33.5	-	-	6.0	1.7	-	6.15

2.2 Sample Preparation

Based on the previous research results (Yang et al. 2022a, 2022b), the ratio of CUCG to GGBFS powder was 6:4, and the water to binder was 0.45. The geopolymers activated by SH activator (2mol/L NaOH), SS activator (18% alkali, Na_2SiO_3 modulus of 0.8) and SSG activator (6% desulfurization gypsum, 16% Na_2SiO_3 and NaOH, Na_2SiO_3 modulus of 0.6) exhibited high compressive and flexural strengths. Therefore, geopolymers were prepared by using these three activators, and their freeze-thaw resistance was studied. The preparation process of the test block was as follows: First, the alkali activator was prepared in the beaker and stirred with a magnetic stirrer for 30 minutes. Then CUCG and GGBFS were placed into the stirring pot, added with the prepared alkali activator solution and stirred with the mixer for 120 s. After that, the slurry was poured into the triple mold (40mm×40mm×160mm), shaken on a vibrating table for 60 times, before being transported to a standard curing room (20±2℃, humidity⩾95%). After curing for 24 hours, the specimen was demolded and continued curing to the specified times (ISO, 2009). Figure 1 shows the preparation process of test blocks.

(a) (b) (c) (d) (e) (f)

Figure 1. Test block preparation process. (a) Stirring with a magnetic stirrer. (b) Stirring with a mixer. (c) The slurry is poured into the mold. (d) Vibrating with a vibrating table. (e) Test block after 24 hours of demolding. (f) The curing box.

2.3 Freeze-Thaw Tests

The quick-freezing method was employed for the freeze-thaw tests, and the tests were carried out in the TDRF-2 concrete rapid freeze-thaw test chamber (Figure 2a, Zhejiang Huanan Instrument Equipment Co., Ltd., Zhejiang, China). The tests were conducted following the procedures of G.T.50082 (2009). Specifically, the 24-day curing specimens were soaked in water at a room temperature of (20±2) ℃ for four days. The specimen was then moved out of the water and any water on the specimen surface was wiped out prior to measuring the initial mass of the specimen (m_{0i}) and being subjected to subsequent freeze-thaw cycling. The freezing and thawing temperatures were set at (−18±2) ℃ and at (5±2) ℃, respectively. Every 25 cycles, the appearance, cross-section, mass, and compressive and flexural strength of the test blocks were observed or measured. Six parallel specimens were made for each group of specimens. The freeze-thaw tests were terminated once one of the following conditions was satisfied: The specified number of freeze-thaw cycles was reached; the compressive strength loss rate reached 25%; the mass loss rate of the specimen reached 5%. The single specimen loss rate, average mass loss rate and strength loss rate are calculated according to Eq. 1 to Eq.3. The compressive and flexural strengths of the specimens were measured by an automatic compressive and flexural testing machine (Figure 2b, WYA-300B, Wuxi Xiyi Building Materials Instrument Factory, Wuxi city, China).

$$\Delta m_{ni} = \frac{m_{0i} - m_{ni}}{m_{0i}} \quad [1]$$

$$\Delta m_n = \frac{\sum_{i=1}^{3} \Delta m_{ni}}{3} \times 100 \quad [2]$$

$$\Delta P_n = \frac{P_0 - P_n}{P_0} \quad [3]$$

Where, Δm_{ni} is the mass loss rate of the i^{th} specimen

after n freeze-thaw cycles, %, m_{0i} is the mass of the i^{th} specimen before the freeze-thaw cycle test, g; m_{ni} is the mass of the i^{th} specimen after n freeze-thaw cycles, g; Δm_n is the average mass loss rate of a group of specimens after n freeze-thaw cycles, %; ΔP_n is the strength loss rate, %; P_0 is the strength of the specimen without freeze-thaw cycle, MPa; P_n is the strength of the specimen after freeze-thaw cycles, MPa.

(a) (b)

Figure 2. Freeze-thaw cycle testing instrument and strength testing instrument. (a) TDRF-2 concrete rapid freeze-thaw test chamber. (b) Automatic compressive and flexural testing machine.

2.4 Mineralogical and Microstructural Characterization

After freeze-thaw cycles, part of a specimen was soaked in anhydrous ethanol for 24h, then placed in the oven to dry, and placed in a drying bag for mineralogical and microstructural characterization testing. XRD (D8 Advance, Bruker AXS, Karlsruhe, Germany, the scanning angle is 5°–90°, 8°per minute), FTIR (Nicolet iS5, Thermo Fischer Scientifific Inc., Waltham, MA, USA) and SEM (Zeiss Sigma 500, Zeiss, Oberkochen, Germany) were used to compare and analyze the mineral composition, functional groups, and microscopic morphology of the samples.

3 RESULTS AND DISCUSSION

3.1 Mass and Appearance Observation

During the freeze-thaw cycle of the specimen, the mass loss rate of the specimen was checked once every 25 cycles, and the test was terminated with the mass loss rate reaching 5%. Figure 3 depicts the mass loss rate of geopolymers under different cycle times. After freeze-thaw cycles, with the increased freeze-thaw cycles, the mass loss rate continued to increase. The mass loss rate of SH geopolymer (activated by NaOH) reached 5.9% at 25 cycles, so the experiment was terminated, while the mass loss rates of SS and SSG geopolymers (activated by NaOH + Na_2SiO_3 and NaOH + Na_2SiO_3 + desulfurized gypsum, respectively) were 4% and 4.2% at 50 cycles, respectively, and finally terminated at 75 cycles.

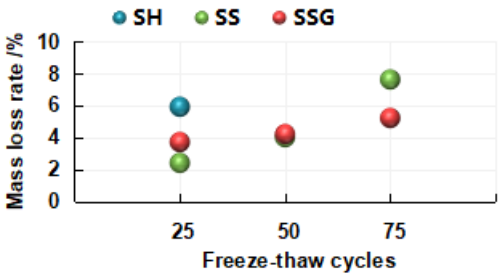

Figure 3. Mass loss rate of geopolymer.

In Figure 4, the external surface and cross-section of the geopolymer changed under different freeze-thaw cycles. All the geopolymers showed damage such as peeling, crisping, and exposed internal specimens after freeze-thaw cycles. And as the number of cycles increased, the damage was severe. As can be seen from Figure 4(a), the SH specimen without circulation had smooth surface, dense cross-section, and dark blue color. However, after 25 cycles, the outer skin of the specimen was completely peeled off, the specimen was crisp, and the color of the section was loose and turned to light gray. The appearance of the non-circulating SS specimen was dark blue with smooth surface and dense cross section in dark blue. With the increase of the number of freezing-thawing cycles, the outer surface was peeled off and the inner specimen was exposed, but the cross section was still dark blue and dense (Figure 4b). In Figure 4(c), the appearance of SSG geopolymer was flat and blue, the cross section was dark blue, and some unreacted desulfurization gypsum could be seen. And at 75 cycles, some of the specimens were broken into two sections, but the sections remained blue and dense.

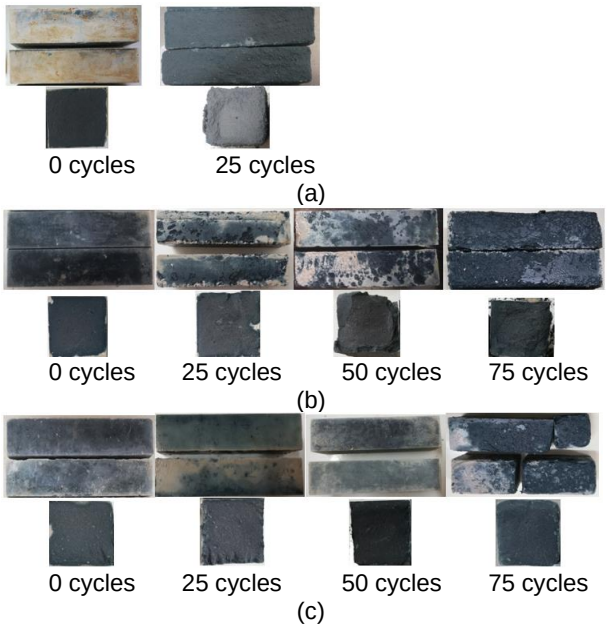

Figure 4. Appearance and cross-section of geopolymer under freeze-thaw cycles. (a) SH geopolymer. (b) SS geopolymer. (c) SSG geopolymer.

3.2 Compressive and Flexural Strengths

After the freeze-thaw cycles of the geopolymer, the strength of the specimens showed varying degrees of loss, and the strength loss gradually increased with the increase of the number of cycles (Figure 5). For different kinds of geopolymers, the geopolymers with higher initial strength have a stronger ability to resist freezing-thawing cycles. SS and SSG geopolymer had higher freezing-thawing resistance, with initial compressive and flexural strengths of 40 MPa and 6 MPa, respectively, which could remain above 35MPa and 4.5MPa after 50 cycles. Followed by SS, the compressive and flexural strengths of SS were 19.6 MPa and 3.6 MPa at 50 cycles. The freeze-thaw cycle resistance of SH was the worst, and the compressive and flexural strengths of 25 cycles were only 13.6MPa and 2.4MPa.

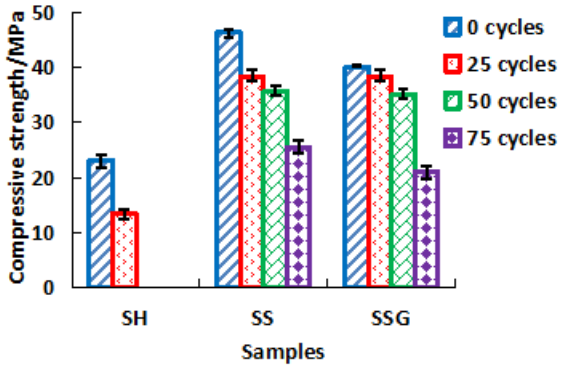

Figure 5. Compressive and flexural strength of geopolymer under different freeze-thaw cycles. (a) Compressive strength. (b) Flexural strength.

Figure 6 describes the intensity change rate. The test should be terminated at the loss rate of the test compressive strength reached more than 25%. Figure 6(a) indicates the change rate of compressive strength ΔPc under freeze-thaw cycles. In 25 cycles, the ΔP_c of SH reached 41.4%, so the freeze-thaw cycle test of SH was terminated. While SS and SSG had lower ΔP_c, 17.7% and 4.5%, respectively. At 50 cycles, the ΔP_c of SS and SSG remained below 25%, and SSG kept a relatively low value of 12.5%. However, the ΔPc of SS and SSG increased significantly, both exceeding 25%, respectively reaching 45% and 47.4% at 75 cycles.

Figure 6(b) shows the change rate of flexural strength ΔP_f under freeze-thaw cycles. At 25 cycles, the ΔP_f of SH geopolymer was 68%, followed by SSG with 29.5%, and the SS with 10.2%. However, the ΔP_f for the SS specimen was 37.2% and some of the SSG specimens fractured at 75 cycles. Through comparative analysis of ΔPc and ΔP_f, the freeze-thaw cycles had a greater influence on the flexural strength of SH and SSG geopolymers, but had a greater impact on the compressive strength of SS.

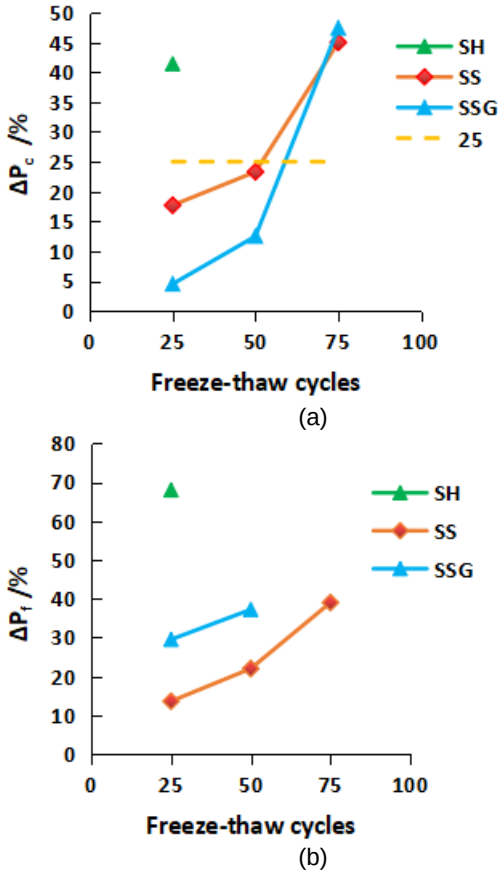

Figure 6. Strength loss rate of geopolymer under different freeze-thaw cycles. (a) Rate of change in compressive strength. (b) Rate of loss of flexural strength.

3.3 Mineral and Microstructure Analyses

3.3.1 XRD

Coal gangue based geopolymers are mainly composed of calcite, SiO_2, sillimanite, analcime, gehlenite, zoisit, gonnardite, thomsonite and mesolite (Figure 7). Sillimanite and analcime are N-A-S-H gel, gehlenite and zoisite belong to C-A-S-H gel, C-N-A-S-H includes gonnardite, thomsonite and mesolite. After the freeze-thaw cycles, the main peak position of the frozen-thawed specimen did not change significantly compared with the unfrozen-thawed

specimen, but the peak value changed, which proved that no new phase was formed, but the content of $CaCO_3$, N-A-S-H, C-A-S-H and C-N-A-S-H decreased correspondingly (the bands in the dotted box in Figure 7). The characteristic peaks of SS and SSG remained obvious after freeze-thaw cycles, and the peaks were higher, which corresponded to their strong freeze-thaw resistance.

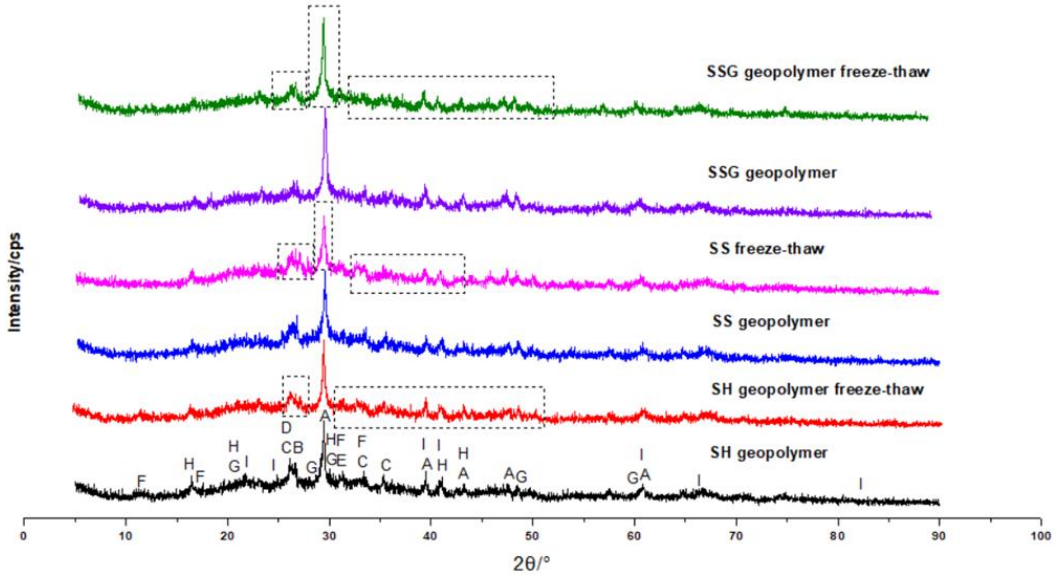

A-Calcite B-SiO_2 C-Sillimanite D-Analcime E-Gehlenite F-zoisite G-Gonnardite H-Thomsonite I-Mesolite

Figure 7. XRD pattern of geopolymer.

3.3.2 FTIR

In Figure 8, the characteristic spectra of the three geopolymers have the same peak positions, which reflects the vibration of the main functional groups in the formation process of geopolymers. The stretching vibration of O−H at 3440−3455cm^{-1} and the bending vibration of H−O−H at 1644−1649cm^{-1} prove that free water and adsorbed water were generated during the polymerization (Yu et al. 1999). The peak at 1426−1447 cm^{-1} is the C−O stretching vibration peak, which is the reaction of carbon dioxide in the air with Ca^{2+} in the polymerization reaction to form calcium carbonate (Ines et al. 2008). The frequency band in the region of 800−1200cm^{-1} is related to the T−O−Si (T=Al, Si) bond formed by TO4, and the shift of the frequency band to a lower frequency proves that the polymerization reaction was relatively violent (Heikal et al. 2014; Ismail et al. 2014). Therefore, the order of the polymerization intensity of SH, SS and SSG geopolymers from high to low is SS>SSG>SH. 400−600cm^{-1} band is Si−O bending vibration (Phair and Van Deventer 2002), 600−800cm^{-1} band is Si−O−Si or Si−O−Al bonds vibration (Yi et al. 2018).

The positions of characteristic bands were consistent with those of uncycled specimens, proving that freeze-thaw cycles did not change the chemical composition of specimens. SH geopolymer, compared with other geopolymers, the absorption peaks of −OH and H−O−H moved to low frequency and the peak intensity decreased, indicating that the free water and adsorbed water in the specimen decreased, which was the main reason for its rapid destruction. In the freeze-thaw cycle experiment, the specimen was isolated from CO_2 in the air by being in water, so the C−O adsorption band moved to the low frequency.

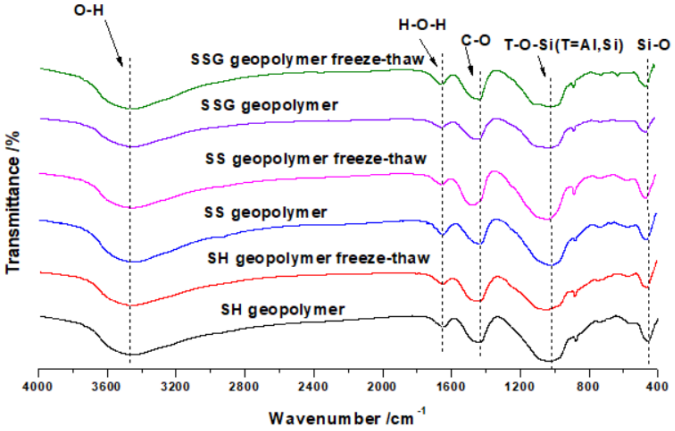

Figure 8. FTIR spectrum of geopolymer.

3.3.3 SEM

Many flocculent, agglomerated, reticulated and flower-like dense gelling substances were formed on the surface of the geopolymer (Figure 9). The appearance of N−A−S−H is cotton-like, C−A−S−H is foil-like and granular (Qin et al.2020), and rod or rod-like minerals are zeolite structure minerals. SH contained a large amount of C−A−S−H gel and N-A-S-H gel (Figure 9a). However, a large number of voids and loose structures appeared in the SH geopolymer

after freeze-thaw cycles, which corresponded to its lower strength (Figure 9b). However, SS and SSG geopolymers produced more crystalline substances, and a lot of zeolite-like structures generated (Figure 9c and Figure 9e). After freeze-thaw cycles, micropores and cracks appeared, but the appearance was still relatively dense, and gels bonded together, consistent with their better resistance to freeze-cycles.

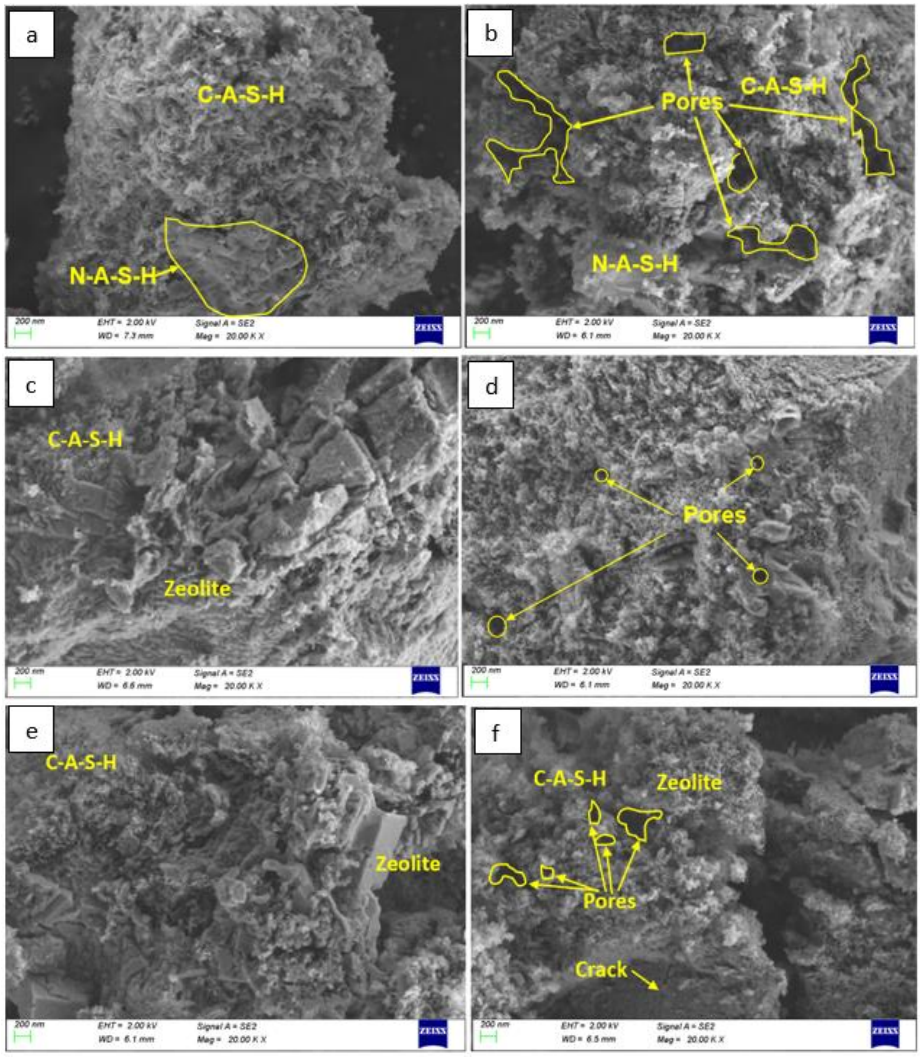

Figure 9. SEM of geopolymer. (a) SH geopolymer (b)SH geopolymer freeze-thaw (c) SS geopolymer (d) SS geopolymer freeze-thaw (e) SSG geopolymer (f) SSG geopolymer freeze-thaw.

Therefore, after the freeze-thaw cycle, all geopolymers did not generate new substances, and the outer surface of the test blocks was damaged and the interior was exposed, and the generated gel became loose, and the voids increased. In the geopolymerization process, water only acted as a reaction medium (to transport the alkali needed in the polymerization process) and did not directly participate in the formation of the final hydration products, which is the main difference from the way of water participation in Portland cement system (Zhao et al. 2019). During the geopolymerization process, the evaporation of water can form harmful pores in the matrix (Krivenko, 1999), which is the fundamental reason for the poor freeze-thaw resistance of geopolymers. During the freeze-thaw cycle, because the test blocks had been immersed in the water of the freeze-thaw box, after the water molecules entered the test blocks, the volume increased due to the frost heave during the frost heave process, and decreased during thawing process, the whole process resulted in the test blocks to became crispy, freeze-broken, and strength loss. Meanwhile, free water and bound water also existed in the specimens after curing for 28 days. During the freeze-thaw process, the form of water changed from liquid to solid for many times, resulting in the breaking of chemical bonds in the gel and the damage of the specimen. Moreover, the freeze-thaw resistance of geopolymers is related to the pore size. SS and SSG geopolymers reacted more violently and rapidly than SH geopolymer, and them

hydration degree was higher. The moisture inside the test blocks was consumed, so their resistance to freeze-thaw cycles were high.

4 CONCLUSIONS

In this study, the appearance change, cross-section, mass and strength change of coal gangue-based geopolymer during freeze-thaw cycles were studied. The mineral and microstructure analyses were carried out by XRD, FTIR, SEM, and the following conclusions were drawn:

(1) Coal gangue-based geopolymers had surface peeling, internal crisping, mass loss, and strength reduction after freeze-thaw cycles.

(2) SS and SSG geopolymers (activated by NaOH + Na_2SiO_3 and NaOH + Na_2SiO_3 + desulfurized gypsum, respectively) had high resistance to repetitive freeze-thaw action, and the compressive and flexural strengths of 50 freeze-thaw cycles could still reach 35MPa and 4.5MPa. SH geopolymer (activated by NaOH) was the weakest against freeze-thaw cycles.

(3) During freeze-thaw cycles, no new phases were formed, while the gels produced were decreased, the pore space increased, and the internal structure was less packed.

(4) SS and SSG geopolymers were highly hydrated and dense with small internal pores, and therefore they had better freeze-thaw resistance than SH geopolymers.

REFERENCES

Bakharev T. 2005. Resistance of Geopolymer Materials to Acid Attack. *Cement and Concrete Research*, 35(4):658-670.

Dos Santos G. Z. B., de Oliveira D.P., Filho. J.D.A.M. et al. 2021. Sustainable Geopolymer Composite Reinforced with Sisal Fiber: Durability to Wetting and Drying Cycles, *Journal of Building Engineerin*g, 43,102568.

Glasby T., Day J., Genrich R., Aldred. J. 2015. EFC Geopolymer Concrete Aircraft Pavements at Brisbane West Wellcamp Airport. *Concrete 2015 Conference*, Melbourne, VIC, Australia,2015:1–9.

G.T.50082, 2009. *Standard for Test Methods of Long-Term Performance and Durability of Ordinary Concrete*, China Architecture & Building Press, Beijing, China, 2009.

Heikal M., Nassar M. Y., G. El-Sayed, et al. 2014. Physico-Chemical, Mechanical, Microstructure and Durability Characteristics of Alkali Activated Egyptian Slag, *Construction and Building Materials,* 69:60-72.

Ilcan H., Sahin O., Kul A., et al. 2022. Rheological Properties and Compressive Strength of Construction and Demolition Waste-Based Geopolymer Mortars for 3D-Printing, *Construction and Building Materials,* 328,127114.

Ines G.L., Fernández-Jiménez, A., Blanco M.T., et al.2008. FTIR Study of the Sol–Gel Synthesis of Cementitious Gels: C–S–H and N–A–S–H, *Journal of Sol-Gel Science and Technol,* 45, 63–72.

Ismail I., Bernal S.A., Provis J. L., et al. 2014. Modification of Phase Evolution in Alkali-Activated Blast Furnace Slag by the Incorporation of Fly Ash, *Cement and Concrete Composites,* 45:125-135.

ISO. 2009. Cement-Test Methods-Determination of Strength, ISO 679:2009(E), International Standards Organization, Geneva, Switzerland.

Kantarci, F. and Maraş M.M. 2022. Fabrication of Novel Geopolymer Grout as Repairing Material for Application in Damaged RC Beams, *International Journal of Civil Engineering,* 20, 461–474.

Krivenko P. 1999. Alkaline Cements: Structure, Properties, Aspects of Durability, *The Proceedings of the Second International Conference on Alkaline Cements and concretes Kiev*, Kiev, Ukraine.

Phair J.W. and Van Deventer J.S.J. 2002. Effect of the Silicate Activator pH on the Microstructural Characteristics of Waste-Based Geopolymers, *International Journal of Mineral Processing,* 66,1-4:121-143.

Qin L., Qu B., Shi C., et al. 2020. Effect of Ca/Si Ratio on the Formation and Characteristics of Synthetic Aluminosilicate Hydrate Gels, *Materials Reports,* 34,6:12058-12064.

Rligh R. and Glasby T. 2013. Development of Geopolymer Precast Floor Panels for the Global Change Institute at University of Queensland. *Proceedings of the Concrete Institute of Australia Biennial Conference,* Concrete. Sydney. NSW. Australia, 2013:1-7.

Sun Q., Li B., Wang H. et al., 2022. Degradation Mechanism and Life Prediction of Tailings and Waste Rock Aggregate Geopolymer Concrete under Freeze-Thaw Corrosion, *Materials Research Express,* 9:015506.

Yang X., Zhang Y., Lin C. 2022 a. Compressive and Flexural Properties of Ultra-Fine Coal Gangue-Based Geopolymer Gels and Microscopic Mechanism Analysis, *Gels*,8,145.

Yang X., Zhang Y., Lin C. 2022 b. Microstructure Analysis and Effects of Single and Mixed Activators on Setting Time and Strength of Coal Gangue-Based Geopolymers, *Gels*, 8,195.

Yi C., Ma H., Chen H., et al. 2018. Preparation and Characterization of Coal Gangue Geopolymers, *Construction and Building Materials*, 187:318-326.

Yu P., R. Kirkpatrick J., Poe B., et al. 1999. Structure of Calcium Silicate Hydrate (C-S-H): Near-, Mid-, and Far-Infrared Spectroscopy, *Journal of the American Ceramic Society*, 82: 742-748.

Zhao R., Yuan Y., Cheng Z., et al. 2019. Freeze-Thaw Resistance of Class F Fly Ash-based Geopolymer Concrete. *Construction and Building Materials*, 222: 474-483.

Zhu H., Yang S., Li W. et al. 2020. Study of Mechanical Properties and Durability of Alkali-Activated Coal Gangue-Slag Concrete, *Materials*, 13(23),5576.

ACKNOWLEDGMENTS

The authors are grateful for the financial support from the China Scholarship Council (202008150091).